IL NUOVO CIMENTO **43 C** (2020) 23
DOI 10.1393/ncc/i2020-20023-6

COLLOQUIA: IFAE 2019

New model-dependent analyses including DAMA/LIBRA–phase2

R. BERNABEI(1)(2), P. BELLI(1)(2), F. CAPPELLA(3)(4), V. CARACCIOLO(5), R. CERULLI(1)(2), C. J. DAI(6), A. D'ANGELO(3)(4), A. DI MARCO(2), H. L. HE(6), A. INCICCHITTI(3)(4), X. H. MA(6), V. MERLO(1)(2), F. MONTECCHIA(2)(7), X. D. SHENG(6) and Z. P. YE(6)(8)

(1) *Dipartimento di Fisica, Università di Roma "Tor Vergata" - Roma, Italy*
(2) *INFN, Sezione di Roma "Tor Vergata" - Roma, Italy*
(3) *Dipartimento di Fisica, Università di Roma "La Sapienza" - Roma, Italy*
(4) *INFN, Sezione di Roma - Roma, Italy*
(5) *INFN, Laboratori Nazionali del Gran Sasso - Assergi (AQ), Italy*
(6) *Key Laboratory of Particle Astrophysics, Institute of High Energy Physics Chinese Academy of Sciences - Beijing, China*
(7) *Dipartimento di Ingegneria Civile e Ingegneria Informatica Università di Roma "Tor Vergata" - Roma, Italy*
(8) *University of Jinggangshan - Ji'an, Jiangxi, China*

received 8 June 2020

Summary. — The first DAMA/LIBRA–phase2 model-independent results (exposure: 1.13 ton $\times$ yr, and software energy threshold at 1 keV) have recently been released. They further confirm —with high confidence level— the evidence already observed by DAMA/NaI and DAMA/LIBRA–phase1 on the basis of the exploited model-independent Dark Matter (DM) annual modulation signature. The total exposure above 2 keV of the three experiments is 2.46 ton $\times$ yr. Several DM candidate particles and related scenarios have been analyzed including the latest results. These analyses permit to constrain the parameters' space of the considered candidates in the given scenarios, restricting their values with respect to previous analyses thanks to the increased exposure and to the lower energy threshold.

1. – Introduction

Recently the model-independent results of the first six full annual cycles measured by DAMA/LIBRA–phase2 with a software energy threshold of 1 keV(1) [1, 2] have been

(1) Throughout this paper: i) keV means keV electron equivalent, where not otherwise specified; ii) ton means metric ton (1000 kg).

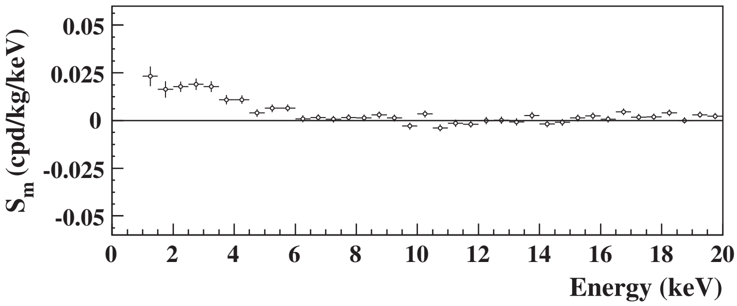

Fig. 1. – Modulation amplitudes, S_m, for the whole data sets: DAMA/NaI, DAMA/LIBRA–phase1 and DAMA/LIBRA–phase2 (total exposure 2.46 ton × yr) above 2 keV; below 2 keV only the DAMA/LIBRA–phase2 exposure (1.13 ton × yr) is available and used. The energy bin ΔE is 0.5 keV. A clear modulation is present in the lowest energy region, while S_m values compatible with zero are present just above.

released [3-7]. The model-independent evidence for the presence of DM particles in the galactic halo is further confirmed on the basis of the exploited DM annual modulation signature after the previous DAMA/LIBRA–phase1 [1, 2, 8-14] and the former DAMA/NaI [15, 16] experiments. The cumulative confidence level is increased from the previous 9.3 σ (data from 14 independent annual cycles for an exposure of 1.33 ton × yr) to 12.9 σ (data from 20 independent annual cycles for an exposure of 2.46 ton × yr).

We recall that the expected DM particles differential counting rate depends on the Earth's velocity in the galactic frame and can be conveniently worked out through a first order Taylor expansion: $\mathcal{S}(t) = \mathcal{S}_0 + \mathcal{S}_m \cos\omega(t - t_0)$, with the contribution from the highest-order terms being less than 0.1%. The $\mathcal{S}_m$ and $\mathcal{S}_0$ are the modulation amplitude and the un-modulated part of the expected signal, respectively, $\omega = 2\pi/T$ with $T = 1$ year and roughly $t_0 \simeq$ June 2nd (when the Earth's speed in the galactic halo is at maximum).

In the DAMA experiments the experimental observable is the modulation amplitude, $\mathcal{S}_m$, as a function of the energy, and the identification of the constant part of the signal, $\mathcal{S}_0$, is not required to point out the presence of a signal in the exploited model-independent annual modulation approach. It has several advantages; in particular, the only background of interest is the one able to mimic the signature, *i.e.*, able to account for the whole observed modulation amplitude and to simultaneously satisfy all its many specific peculiarities [5]. No background of this sort has been found [2-13].

The modulation amplitudes, S_m, for the whole data sets: DAMA/NaI, DAMA/LIBRA–phase1 and DAMA/LIBRA–phase2 (total exposure 2.46 ton × yr) are plotted in fig. 1; the data below 2 keV refer only to the DAMA/LIBRA–phase2 exposure (1.13 ton × yr). It can be inferred that positive signal is present in the (1–6) keV energy interval, while S_m values compatible with zero are present just above [5].

The implications on some models, we already investigated in the past, have been updated by including the data of DAMA/LIBRA–phase2. Here only the results obtained for few models are resumed, see ref. [17] for full information.

2. – Data analysis

In a model-dependent analysis it is important to point out at least the main topics which enter in the determination of the results and the related uncertainties (see ref. [17]

and references therein). Here, to account at some extent for the uncertainties in halo models and to allow direct comparisons, the same not-exhaustive set of halo models as in previous published analyses [15, 16, 18], is considered; they are illustrated in table II of ref. [18].

We also consider the physical ranges of the local velocity v_0: from 170 km/s to 270 km/s, and of the local total DM density, ρ_0; its range is reported in table III of ref. [18] for each considered halo model. Moreover, to take into account that the considered DM candidate can be just one of the components of the dark halo, the ξ parameter is introduced; it is defined as the fractional amount of local density in terms of the considered DM candidate ($\xi \leq 1$). Thus, the local density of the DM particles is $\rho_{DM} = \xi\rho_0$. Finally, the DM escape velocity $v_{esc} = 550$ km/s is adopted as often considered in literature (no sizable differences are observed in the final results when v_{esc} values ranging from 550 to 650 km/s are considered).

In the case of DM particles inducing nuclear recoils the detected energy was evaluated according to the following three instances [17]: i) Na and I quenching factors "constants" with respect to the recoil energy: $q_{Na} = 0.3$ and $q_I = 0.09$ [19] (case (Q_I)); ii) quenching factors depending on recoil energy, evaluated as in ref. [20] (case (Q_{II})); iii) including the channeling effect according to the procedure given in ref. [21]. Finally, three discrete set of values A, B and C are considered in the following to account for possible uncertainties on the quenching factors measured by DAMA in its detectors and on the parameters used in the SI and SD nuclear form factors (see ref. [17] for details).

In conclusion, the allowed regions in the parameters' space of each considered scenario can be derived by comparing —for each k-th energy bin of 1 keV— the measured DM annual modulation amplitude, $\mathcal{S}^{exp}_{m,k} \pm \sigma_k$ with the theoretical expectation in each considered framework, $\mathcal{S}^{th}_{m,k}$. Of course, the $\mathcal{S}^{th}_{m,k}$ values depend on the free parameters of the model $\bar{\theta}$, such as the DM particle mass, the cross section, etc., on the uncertainties accounted for, on the proper accounting for the detector's features, and on priors. In particular, a cautious prior on $\mathcal{S}_{0,k}$ —assuring safe and more realistic allowed regions/volumes— was worked out from the measured counting rate in the cumulative energy spectrum for DAMA/LIBRA–phase2 [17]: $\mathcal{S}_0 \lesssim 0.80$ cpd/kg/keV in the (1–2) keV energy interval; $\mathcal{S}_0 \lesssim 0.24$ cpd/kg/keV in (2–3) keV, and $\mathcal{S}_0 \lesssim 0.12$ cpd/kg/keV in (3–4) keV. These priors on $\mathcal{S}_{0,k}$ have been included in the evaluation of the χ^2 of each considered model [17]. Thus, the calculated χ^2 for each considered model is function of the model parameters $\bar{\theta}$ and we can define: $\Delta\chi^2(\bar{\theta}) = \chi^2(\bar{\theta}) - \chi^2_0$ where χ^2_0 is the χ^2 for $\bar{\theta}$ values corresponding to absence of signal. The $\Delta\chi^2$ is used in the following to determine the allowed intervals of the model parameters $\bar{\theta}$ at 10 σ from the *null signal hypothesis*.

3. – Updated corollary model-dependent scenarios

3·1. *DM particles elastically interacting with target nuclei.* – A lot of candidates have been proposed in theory extending the Standard Model of particles that includes candidates for DM elastically scattering off target nuclei. The cross section is given by the sum of two contributions: the SI and the SD one. The regions allowed by DAMA experiments for the purely SI and for the purely SD scenarios in the considered model frameworks have been calculated and are shown in fig. 2 (see ref. [17] for the mixed SI-SD case). The regions are reported in the nucleon cross section ($\xi\sigma_{SI}$ or $\xi\sigma_{SD}$) *vs.* DM particle mass (m_{DM}) plane. In the case of SD interaction a further parameter must be introduced [22]: $\tan\theta = \frac{a_n}{a_p}$, where $a_{p,n}$ are the effective DM-nucleon coupling strengths

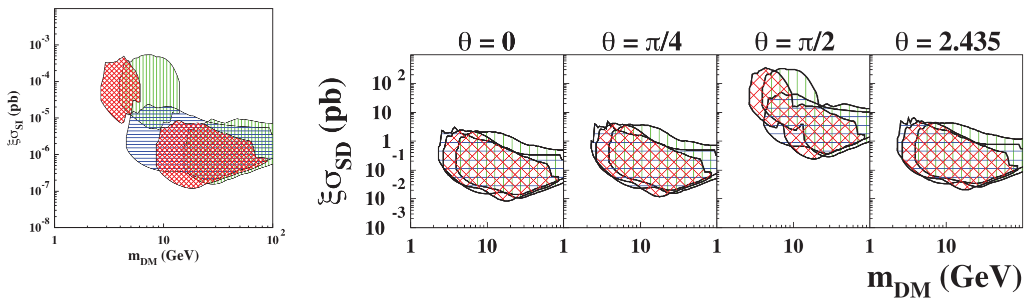

Fig. 2. – Regions —allowed at 10 σ from absence of signal— in the nucleon cross section *vs.* DM particle mass plane allowed by DAMA experiments in the case of a DM candidate elastically scattering off target nuclei and purely SI (left) or purely SD (right) interaction. Three different instances for the Na and I quenching factors have been considered: i) Q_I case (green vertically hatched region), ii) with channeling effect (blue horizontally hatched region) and iii) Q_{II} (red cross-hatched region).

for SD interactions. The mixing angle θ is defined in the $[0, \pi)$ interval; in particular, θ values in the second sector account for a_p and a_n with different signs. See ref. [17] for further details (*e.g.*, on the assumed form factors, scaling laws, etc.).

The results of the analysis for a single halo model hypothesis for the case of a DM candidate with SI isospin violating interaction are reported in fig. 3, where the allowed regions in the f_n/f_p *vs.* m_{DM} plane are shown after marginalizing on $\xi\sigma_{SI}$; f_p and f_n are the effective DM particle couplings to protons and neutrons, respectively. Obviously the previous case of isospin conserving is restored whenever the ratio $f_n/f_p = 1$.

In conclusion, both the purely SI and the purely SD scenarios are supported by the data for low- and high-mass candidates. The same hold also in the case of isospin violating SI interaction for a wide range of the ratio f_n/f_p. See ref. [17] for more details.

3˙2. *Inelastic dark matter*. – Another scenario regards the inelastic DM [23-26]. In this case the DM particles can only inelastically scatter off nuclei going to excited levels with a δ mass splitting. It has been shown [23] that a kinematic constraint exists which favors

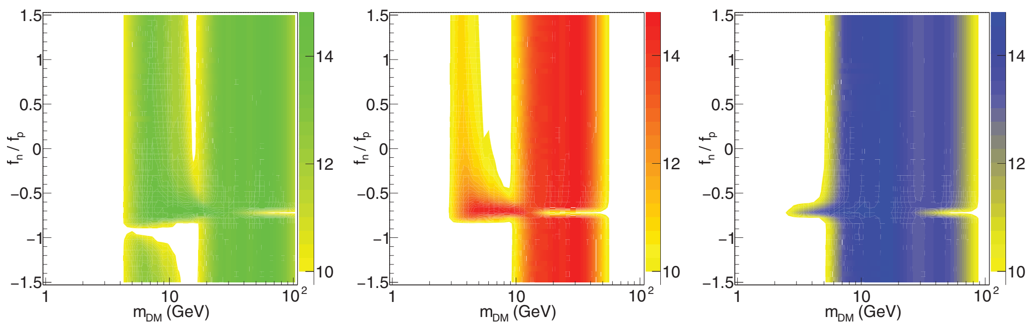

Fig. 3. – Regions in the f_n/f_p*vs.* m_{DM} plane allowed by DAMA experiments in the case of a DM candidate having isospin violating SI interaction. The Na and I quenching factors are: Q_I (left, green), Q_{II} (center, red), and with channeling effect (right, blue). The considered halo is A0 (isothermal sphere) with the v_0 and ρ_0 in the range of table III of ref. [18]. The three possible sets of parameters A, B and C are considered (see sect. **2**). The color scales give the confidence level in units of σ from the *null hypothesis*.

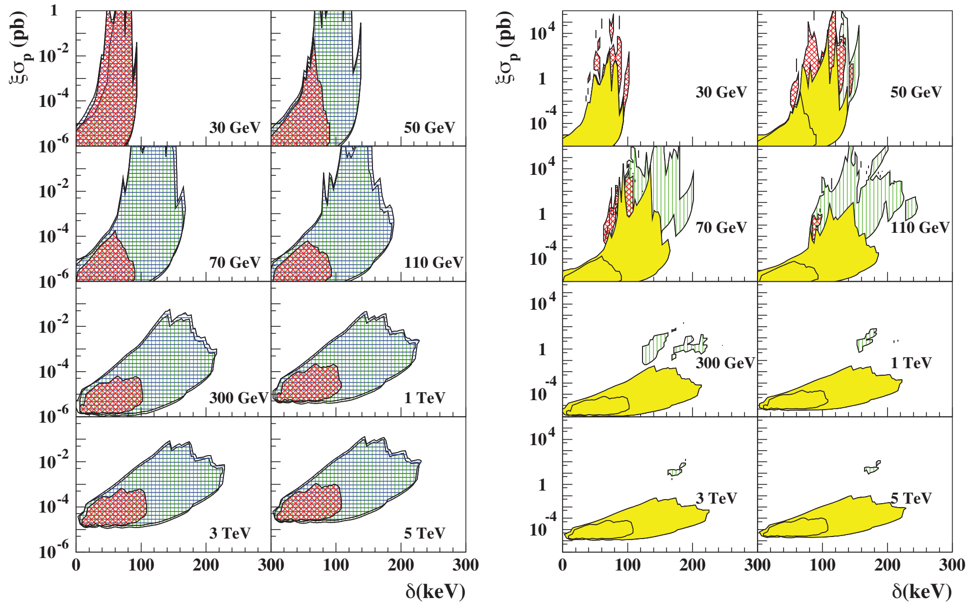

Fig. 4. – Slices of the 3-dimensional volume $(\xi\sigma_p, \delta, m_{DM})$ allowed by DAMA experiments in the case of a DM candidate with preferred inelastic interaction. Three different instances for the target nuclei quenching factors have been considered: i) Q_I case (green vertically hatched region), ii) with channeling effect (blue horizontally hatched region) and iii) Q_{II} (red cross-hatched region). In the right plots the inelastic scattering off thallium nuclei is also included; here the regions due to inelastic scattering only off Na and I nuclei, already shown on the left, are reported in (yellow) light-filled.

heavy nuclei with respect to lighter ones as target-detectors media. Slices of the DAMA allowed 3-dimensional volume in the space ($\xi\sigma_p$, m_{DM}, δ) is reported in fig. 4(left) for the case of sodium and iodine nuclei. Figure 4(right) shows that new regions are allowed by DAMA when even the presence of the thallium dopant in NaI(Tl) detectors is taken into account. Such regions are not fully accessible to detectors with target nuclei having mass lower than thallium. See ref. [17] for more details.

3˙3. *Corollary analysis for other DM candidate particles*. – Several other model dependent scenarios were considered in the corollary analysis of the DAMA data. In particular:

- DM particles with preferred electron interaction, provided by some extensions of the standard model. Such DM candidate particles can be directly detected only through their interaction with electrons in the detectors of a suitable experiment, while they cannot be studied when subtraction/rejection of the electromagnetic component of the experimental counting rate is applied.

- Light dark matter, DM candidate particles with sub-GeV mass provided by some extensions of the Standard Model. Several LDM candidates have been proposed in Warm DM scenarios, as keV-scale sterile neutrino, axino, gravitino, and MeV-scale particles (see ref. [27] for details). DAMA has investigated the direct detection of LDM candidate particles considering the possible inelastic scattering channels either off the electrons or off the nuclei of the target.

- Well-motivated DM candidates are represented by the so-called Mirror particles. The Mirror scenario can be introduced by considering a parallel gauge sector with particle physics exactly identical to that of ordinary particles, coined as mirror world. In this theory the Mirror particles belong to the hidden or shadow gauge sector and can constitute the DM particles of the Universe. A comprehensive discussion about Mirror Matter as DM component can be found in refs. [28, 29].

All the analyses updated by including the new data of the first six annual cycles of DAMA/LIBRA–phase2 with lower software energy threshold are reported in ref. [17].

4. – Conclusions

A high confidence level model-independent evidence for the presence of DM particles in the galactic halo has been achieved by DAMA/NaI, DAMA/LIBRA–phase1 and by the first six full annual cycles of DAMA/LIBRA–phase2 on the basis of the exploited signature.

The DAMA/LIBRA–phase2 data, collected over the first six full annual cycles ($1.13\,\text{ton} \times \text{yr}$) with a software energy threshold down to 1 keV, are analyzed with the DAMA/NaI and DAMA/LIBRA–phase1 data for several scenarios for DM candidates [17]. Several scenarios are compatible with the observed signal; other possibilities are open as well.

The new data have allowed significantly improving the confidence levels and restricting the allowed parameters' space for the various considered scenarios with respect to previous DAMA analyses. It shows how important is to improve the capability of the experiment to effectively disentangle among the many possible different scenarios. For such a purpose an increase of exposure in the new lowest energy bins and the lowering of the software energy threshold below 1 keV are important. Thus, DAMA/LIBRA–phase2 has continued its data taking and R&D's towards the so-called phase3 have been funded and are in progress.

REFERENCES

[1] Bernabei R. *et al.*, *J. Instrum.*, **7** (2012) P03009.
[2] Bernabei R. *et al.*, *Int. J. Mod. Phys. A*, **28** (2013) 1330022.
[3] Bernabei R. *et al.*, *Universe*, **4** (2018) 116.
[4] Bernabei R. *et al.*, *Bled Workshops Phys.*, **19 n.2** (2018) 27.
[5] Bernabei R. *et al.*, *Nucl. Phys. At. Energy*, **19** (2018) 307.
[6] Bernabei R. *et al.*, *Nucl. Part. Phys. Proc.*, **303–305** (2018) 74.
[7] Bernabei R. *et al.*, in *Proceeding of the 15-th Marcel Grossmann Meeting* (World Scientific, Singapore) 2019.
[8] Bernabei R. *et al.*, *Nucl. Instrum. Methods Phys. Res. A*, **592** (2008) 297.
[9] Bernabei R. *et al.*, *Eur. Phys. J. C*, **56** (2008) 333.
[10] Bernabei R. *et al.*, *Eur. Phys. J. C*, **67** (2010) 39.
[11] Bernabei R. *et al.*, *Eur. Phys. J. C*, **73** (2013) 2648.
[12] Bernabei R. *et al.*, *Eur. Phys. J. C*, **72** (2012) 2064.
[13] Bernabei R. *et al.*, *Eur. Phys. J. C*, **74** (2014) 3196.
[14] DAMA Collaboration, *Int. J. Mod. Phys. A*, **31** (2016) issue dedicated to DAMA.
[15] Bernabei R. *et al.*, *Riv. Nuovo Cimento*, **26 n.1** (2003) 1.
[16] Bernabei R. *et al.*, *Int. J. Mod. Phys. D*, **13** (2004) 2127.
[17] Bernabei R. *et al.*, arXiv:1907.06405.
[18] Belli P. *et al.*, *Phys. Rev. D*, **66** (2002) 043503.

[19] Bernabei R. *et al.*, *Phys. Lett. B*, **389** (1996) 757.
[20] Tretyak V. I., *Astropart. Phys.*, **33** (2010) 40.
[21] Bernabei R. *et al.*, *Eur. Phys. J. C*, **53** (2008) 205.
[22] Bernabei R. *et al.*, *Phys. Lett. B*, **509** (2001) 197.
[23] Smith D. and Weiner N., *Phys. Rev. D*, **64** (2001) 043502.
[24] Tucker-Smith D. and Weiner N., *Phys. Rev. D*, **72** (2005) 063509.
[25] Finkbeiner D. P. *et al.*, *Phys. Rev. D*, **80** (2009) 115008.
[26] Bernabei R. *et al.*, *Eur. Phys. J. C*, **23** (2002) 61.
[27] Bernabei R. *et al.*, *Mod. Phys. Lett. A*, **23** (2008) 2125.
[28] Addazi A. *et al.*, *Eur. Phys. J. C*, **75** (2015) 400.
[29] Cerulli R. *et al.*, *Eur. Phys. J. C*, **77** (2017) 83.